The $He + H_2^+ \rightarrow HeH^+ + H$ reaction: *Ab initio* studies of the potential energy surface, benchmark time-independent quantum dynamics in an extended energy range and comparison with experiments

Dario De Fazio,[1,2,a)] Miguel de Castro-Vitores,[3] Alfredo Aguado,[4] Vincenzo Aquilanti,[1,5] and Simonetta Cavalli[5]

[1]*Istituto di Metodologie Inorganiche e dei Plasmi - C.N.R., 00016 Roma, Italy*
[2]*IKERBASQUE, Basque Foundation for Science, E-48011 Bilbao, Spain*
[3]*Departamento de Medio Ambiente - B.V.B.S., 28108 Madrid, Spain*
[4]*Departamento de Química Física Aplicada, Universidad Autónoma de Madrid, 28049 Madrid, Spain*
[5]*Dipartimento di Chimica, Università di Perugia, 06123 Perugia, Italy*

(Received 12 August 2012; accepted 3 December 2012; published online 28 December 2012)

In this work we critically revise several aspects of previous *ab initio* quantum chemistry studies [P. Palmieri *et al.*, Mol. Phys. **98**, 1835 (2000); C. N. Ramachandran *et al.*, Chem. Phys. Lett. **469**, 26 (2009)] of the HeH_2^+ system. New diatomic curves for the H_2^+ and HeH^+ molecular ions, which provide vibrational frequencies at a near spectroscopic level of accuracy, have been generated to test the quality of the diatomic terms employed in the previous analytical fittings. The reliability of the global potential energy surfaces has also been tested performing benchmark quantum scattering calculations within the time-independent approach in an extended interval of energies. In particular, the total integral cross sections have been calculated in the total collision energy range 0.955–2.400 eV for the scattering of the He atom by the *ortho*- and *para*-hydrogen molecular ion. The energy profiles of the total integral cross sections for selected vibro-rotational states of H_2^+ ($v = 0,\ldots,5$ and $j = 1,\ldots,7$) show a strong rotational enhancement for the lower vibrational states which becomes weaker as the vibrational quantum number increases. Comparison with several available experimental data is presented and discussed. © *2012 American Institute of Physics*. [http://dx.doi.org/10.1063/1.4772651]

I. INTRODUCTION

It is well known that several relevant chemical processes in many gas phase environments, such as the molecular hydrogen plasma occurring in interstellar clouds, planetary ionospheres, ion sources, and thermonuclear experiments, involve ion-molecule reactions (see, e.g., Ref. 1 and references therein). In particular, in the interstellar medium the most important processes are ion-molecule barrier-less reactions because the low temperature switches off the rate constants of many neutral reactions. The non-Arrhenius behavior[2] followed by the rate constants in these regimes is very difficult to be predicted by approximate models because of the relevant role played by resonance mechanisms, so that an extrapolation from the kinetic data at higher temperature can give unreliable results.

The direct ($He + H_2^+ \rightarrow HeH^+ + H$) and inverse ($HeH^+ + H \rightarrow He + H_2^+$) reactions of the HeH_2^+ system have several features that make them important benchmark cases for the ion-molecule class of reactions. The diatomic fragments involved are known theoretically and experimentally at the highest level of accuracy. In fact, the large dipole moment of the HeH^+ molecule has permitted to obtain a large database of spectroscopic transitions with μ-Hartree ($\approx$0.2 cm^{-1}) accuracy (see Ref. 3 and references therein). This database and the small number of electrons involved have permitted to experimentally test the introduction into the electronic Hamiltonian of relativistic[4] and quantum electron dynamics corrections coming from quantum field theory.[5] The simplicity of the HeH_2^+ system makes it an ideal candidate to extend these calculations to triatomic systems and to observe effects beyond the quantum non-relativistic theory in reaction dynamics. Besides being a benchmark theoretical system for the ion-molecule class of reactions, the HeH_2^+ system and its isotopic variants are also important from the astrophysical and cosmological points of view. In particular, the $HeH^+ + H$ reaction is considered of great relevance in the chemical network of the early universe evolution,[6] so that the production of accurate rate constants for this fast exothermic process is crucial for a reliable determination of the abundance of the main molecular species during the gravitational collapse which led to the formation of the first stars.[7]

However, to achieve realistic quantum dynamical results in the cold astrophysical regimes and to test fine effects into the electronic Hamiltonian, a highly accurate Born-Oppenheimer (BO) description of the potential energy surface (PES) is an unavoidable crucial step. Although state-of-the-art quantum chemistry calculations allow one to reach spectroscopic accuracy (within 1 cm^{-1}) and beyond, at least in some local regions of the simplest triatomic systems,[8,9] the accuracy of the global PES, required in dynamical studies, is often very difficult to be estimated. It depends on several factors such as the extension of the one-electron basis set used in quantum chemistry calculations, the number and the distribution of the triatomic configurations selected, the accuracy of the *ab initio* method employed to treat the

a)defazio.dario@yahoo.it.

multielectron correlation energy, and the flexibility of the analytical functional form used to fit the data. Moreover, the long-range part of the interaction potential, which strongly influences the rate of fast ionic reactions, is difficult to be described by *ab initio* calculations and by the most common analytical functional forms employed. In this case, semiempirical methods exploiting correlation and perturbative formulas in terms of fundamental physical properties of the interacting partners can be applied (for recent applications to charged systems see Refs. 10 and 11). Therefore, a reliable estimate of the accuracy of the PES eventually comes from direct comparison with the experimental data, where they are available. Care must of course be payed for additional sources of uncertainty coming from the experimental errors and the approximations introduced in the treatment of the nuclear dynamics.

From the dynamical point of view, several difficulties arise in the calculations of these processes. A deep potential well (of the order of magnitude of 0.35 eV at the collinear geometry) near to the reactants' valley[12] gives rise to a large number of metastable resonance states producing relevant quantum effects.[13] The relevance of the Coriolis coupling[14] makes large the number of projections of the total angular momentum to be included into the dynamical calculations, thus increasing drastically the complexity of the algebraic problem. Moreover, because of the electric charge, the number of partial waves required to obtain convergent results is larger than for neutral systems making the calculations more difficult, and much more time consuming. Therefore, notwithstanding the lightness of the atoms involved in the HeH_2^+ system, only a few benchmark time-independent calculations have been carried out in a narrow interval of collision energies close to the reaction threshold.[12,15] In fact, most of the dynamics calculations have been performed using classical trajectories or approximate quantum mechanical methods of dubious reliability considering the lightness of the species involved and the pronounced resonance energy pattern of the system.[13] More recently, wave-packet quantum mechanical calculations including Coriolis coupling have been performed in a wide range of collision energies, for the $He + H_2^+$ reaction[16] and the isotopic variant $He+HD^+$.[17] However, the small number of total angular momentum projections used in that work and the well known relevance of Coriolis coupling for these systems,[12,14,16,18] do not allow us to classify these results as benchmark data. Moreover, the analysis presented in Ref. 16 shows significant differences with other wave-packet results[19] performed with the same PES, so that more reliable time-independent studies are desirable.

The experimental determination of the reactive observables suffers as well from important specific problems. Most of the atomic and molecular species involved are unstable in nature so that it is not easy to obtain molecular beams of pure reactants. Moreover, Coulomb repulsion among charges makes it difficult the production of narrow, focused molecular beams of ions at low collision energies and specific devices must be used to get control of the ion collision energy.[20] Because of these difficulties, the available experimental results have generally poor rotational and translational energy resolution, thus smearing the rich resonance pattern of the reaction.

The studies of the HeH_2^+ system have a long history and several significant papers have been published in the literature. It is not our intention to give in this article an exhaustive review of the work done so that we comment just those providing, in our opinion, the most relevant advancements. Further important works can be found in the bibliography of the references cited in this introduction. Historically, the PES most used in dynamical calculations has been that of Joseph and Sathyamurthy,[21] obtained fitting the *ab initio* energies (a set of 596 values calculated by McLaughlin and Thompson[22] applying the multi-configuration self-consistent field theory) by a Sorbie-Murrel functional. The accuracy of the quantum chemistry calculations was estimated to be within the root-mean-square deviation of the analytical fitting (around 50 meV). The reason of the success of this PES was that for the first time the *ab initio* points were calculated at internuclear geometries different from the collinear configuration. Later, this set of energies has been used in Ref. 23 to obtain an alternative analytical fit of the PES with root-mean-square deviation similar to Ref. 21. Classical trajectories[24] and approximate quantum mechanical treatments[13] have shown a large sensitivity of the reactive observables, and in particular of the resonance energy pattern, to the analytical fitting employed.

Significant improvement in the description of the intermolecular interaction was achieved in Ref. 12 where about 1500 energies were calculated at the multi-reference configuration interaction (MRCI) level. The functional form of Ref. 23 was employed for the analytical fits obtaining root-mean-square deviations of the order of a few tens of meV. Different degrees of the polynomials were used to investigate the sensitivity of the close-coupling quantum dynamical calculations[25] to the accuracy of the fitting. To improve the description of reaction dynamics, a high density of internuclear geometries was selected in the regions of the configuration space where the effective potentials as a function of the hyperradius exhibited many avoided crossings. These regions were identified generalizing previous hyperspherical studies[26–28] performed on collinear reactions that have indicated that most of the reactive avoided crossings were localized along the hyperspherical ridge separating the valleys of the reactants and of the products. However, only few experimental data[29] were available at the time in the narrow energy range covered by the dynamical calculations, so that the actual improvement in the PES description was not fully demonstrated by the dynamical results of Ref. 12.

Afterwards, the comparison of new experimental data[30] with the time-dependent quantum mechanical calculations[16] carried out on the PES of Ref. 12 has shown a good agreement, thus demonstrating the reliability of the PES and of the strategy used to choose the set of the internuclear geometries. To further investigate the relevance of the method used in the electronic structure calculations, the same set of configurations has been later used in a full-configuration interaction (Full CI) calculation.[31] These points were fitted using the functional form of Ref. 23 to obtaining a PES with a root-mean-square deviation lower than that of the PESs of Ref. 12.

More details about these PESs will be given in Sec. II. Although several classical trajectories,[32] stereodynamical,[33] and approximated quantum dynamical studies[34,35] have already been performed with the PESs of Ref. 31, rigorous quantum dynamical calculations were still lacking, so it was not clear whether these PESs really improve the agreement with the experimental data. The aim of this work is therefore to fill this gap performing new time-independent quantum reactive scattering calculations in the wide collision energy range covered by the experiments.

The article is organized as follows. In Sec. II, several aspects of the PESs of Refs. 12 and 31 will be analyzed and, in the Appendix, the diatomic frequencies will be compared with highly accurate theoretical and spectroscopic data. In Sec. III, we report details of the quantum reactive scattering calculations, describing convergence tests and the improving of the computer code that has permitted to enlarge the investigated collision energy range with respect to previous studies. In Sec. IV, the integral cross sections obtained with some analytical fits of Refs. 12 and 31 will be reported and compared among them and with the available experimental data, to test the reliability of the description of the intermolecular interactions. The results obtained will be analyzed in Sec. V. Finally, we report our conclusions in Sec. VI.

II. THE POTENTIAL ENERGY SURFACES

As mentioned in the Introduction, a dozen years ago, accurate quantum chemistry calculations were performed for the title reaction.[12] In that work, 1727 *ab initio* energies were evaluated using the multi-reference configuration interaction method, as implemented in the MOLPRO suite of programs.[36] The basis set employed was the correlation-consistent polarized valence cc-p V5Z of Dunning.[37] An original feature of this work was the choice of the internuclear geometries where the quantum chemistry calculations were performed. Instead to use, as usual, an evenly spaced grid in the internuclear distances, a suitably spaced grid in hyperspherical coordinates was employed. In particular, many points were taken along the hyperspherical ridge of the reaction (the hyperradial line of separation between reactants and products valley), and in the neighborhood of other critical points of the PES, which were expected to be more sensitive to the reaction dynamics.

From this set of *ab initio* energies, a subset of 1487 geometries were used for the generation of PESs. The criterion used to select these geometries was mainly based on energy considerations: all the geometries corresponding to energy values 1 eV above the triatomic dissociation limit were excluded. The reason for this choice was that higher energies were expected to be of lower accuracy because of the possible interference of excited electronic states and thought to be not relevant for the reaction dynamics of the ground PES at low and moderate collision energies. In addition, a small set of less reliable internuclear geometries was also excluded because a problematic convergence behavior was observed in the MOLPRO calculations. The analytical fits were made using a many-body expansion

$$V = V_1(r_1) + V_2(r_2) + V_3(r_3) + V_{123}(r_1, r_2, r_3). \quad (1)$$

Following the work of Ref. 23, the triatomic interaction polynomial V_{123} was taken as

$$V_{123} = \sum_{i,j,k}^{M} d_{ijk}\, x_{12}^{i}\, x_{23}^{j}\, x_{13}^{k} \quad i + j + k \neq i \neq j \neq k \leq M, \quad (2)$$

with M being the degree of the polynomial expansion and

$$x_{ij} = r_{ij} e^{-\beta_{ij} r_{ij}}, \quad i, j = 1, 2, 3 \quad (3)$$

are Rydberg functions.

Three PESs with $M = 6$, 10, and 12 were generated to test the sensitivity of the reaction dynamics with respect to the accuracy of the analytical fit. Hereafter, we will call these PESs PM6, PM10, and PM12 (Palmieri $M = 6$, 10, and 12), respectively. However, because of the limitation on the number of the optimized coefficients imposed by the version of the fitting program[38] available at the time, just the additional linear coefficients of each PES were permitted to change, keeping fixed the parameters of the Rydberg functions and the coefficients of the lower order polynomials. In this way, it was possible to obtain an analytical fit for $M = 12$ with a root-mean-square deviation of about 12 meV. With this PES, quantum reactive scattering time-independent calculations were performed at collision energies up to 200 meV above the reactive threshold. However, because of an error in the implementation into the fitting program of the coefficients of highest order, PM12 PES is not perfectly symmetric with respect to the hydrogen exchange as it should be. This unphysical behavior is not present in the fits of lower order (PM6 and PM10).

In view of this drawback and to test the accuracy of the quantum chemistry *ab initio* method employed to treat the multi-electron correlation energy, further work[31] has been done subsequently. In that work, the same set of 1727 internuclear geometries has been used to generate *ab initio* energies at Full CI level of theory and new diatomic curves were also generated. However, to reduce the computational effort a basis set of lower extension (namely a Dunning cc-p VQZ) was employed. All the energy points (1511 geometries) below the triatomic dissociation energy were fitted to the analytical form in Eqs. (1)–(3), optimizing simultaneously all coefficients and directly implementing the exchange symmetry in the functional. We note that, although just a small number of geometries change (about 5%) with respect to the subset used in Ref. 12, the stricter criterion chosen could give important differences in the repulsive three body region where no geometries were selected. In this case, the degree of the polynomial was limited to $M = 8$ to avoid unphysical behaviors appearing in the repulsive region of the PES, when larger values of M were used to simultaneously optimize the coefficients of the PES. Also, MRCI calculations with the same basis set used in Ref. 12 were repeated using an updated version of the MOLPRO package and the points were used to generate the analytical fit with the same procedure employed for the Full CI energies. The two new global PESs generated, hereafter denominated RFCI (Ramachandran Full CI) and RMRCI (Ramachandran MRCI) PESs, have a root-mean-square deviation of 6 and 7 meV for the Full CI and MRCI fitting, respectively. In spite of the lower root-mean-square devia-

tions, the new surfaces cannot be considered "*a priori*" an improvement with respect to the PESs of Ref. 12 because of the different extension of the one-electron basis set employed and of the minor differences in the subsets of internuclear geometries effectively used in the fitting procedure. Only the comparison of the dynamical observables with the experimental data can give some indication on the accuracy of the description of the interaction, and this is a main objective of the present work.

A. The diatomic curves

In order to assess the accuracy of the diatomic energy terms of Eq. (1) in the PESs of Refs. 12 and 31, the diatomic potential energy curves, PECs, have been calculated varying the extension of the basis set employed. For H_2^+ and HeH^+, for which only single and double excitations are possible, MRCI and Full CI calculations are mathematically equivalent so that differences can only be attributed to the different extension of the one-electron basis set used. In particular, we have used augmented correlation consistent polarized basis sets of Dunning (aug-cc-pV5Z and aug-cc-pV6Z) and obtained the extrapolation to the complete basis set (CBS) limit using the methodology of Ref. 39. In this way 105 and 102 energies were obtained for the H_2^+ and the HeH^+ cations, respectively, and fitted with the following functional form:[9]

$$V(r) = c_0 \frac{\exp(-\alpha r)}{r} + \sum_{i=1}^{L} c_i x^i(r) + V_{\text{long}}(\tilde{r}), \qquad (4)$$

where $x(r) = r\exp(-\beta r)$.

The leading terms in the long-range interaction V_{long} between a proton and an atom in a S state can be written as

$$V_{\text{long}}(r) = -\frac{1}{2}\alpha_0 r^{-4} - \left[\frac{1}{2}\alpha_q + C_6\right] r^{-6}, \qquad (5)$$

where α_0 and α_q are dipole and quadrupole polarizabilities of the atom, respectively, and C_6 represents the dispersion coefficient. For the He(^{2}S) ground state, the dipole polarizability obtained with the aug-cc-pV5Z basis set is 1.383 06 a.u., comparable with the best theoretical result, 1.383 173 94 a.u.[40] The quadrupole polarizability and C_6 dispersion constant obtained are 2.233 and 2.082 a.u., respectively, comparable with 2.444 and 2.083 a.u. used in Refs. 41 and 42. For the H(^{2}S) ground state we have used the long-range terms of Ref. 9.

Finally, to eliminate the divergence of the long range terms at short distances, we scale the independent variable as[9]

$$\tilde{r} = r + r_0 \exp(-(r - r_e)), \qquad (6)$$

where r_0 is a distance parameter selected to give the correct long-range behavior, and r_e is the equilibrium distance. Parameter free damping functions[43] could also be employed but this requires the calculation of the atomic ground state electronic density and more computational effort is needed. The obtained root-mean-square deviations were 0.0042 and 0.013 meV for the H_2^+ and the HeH^+ ions, respectively, and the largest differences between fitted and calculated energy values were 0.011 and 0.043 meV.

TABLE I. Equilibrium distances (R_e), dissociation energies (D_e), and number of bound vibrational levels (N_v) of the ground electronic states of HeH^+ and H_2^+ using different diatomic curves and theoretical methods.

	HeH^+			H_2^+		
PEC	R_e (a_0)	D_e (eV)	N_v	R_e (a_0)	D_e (eV)	Nv
PM[a]	1.4630	2.0259	10	1.9929	2.7847	18
RFCI[b]	1.4639	2.0430	11	1.9982	2.7910	18
RMRCI[b]	1.4634	2.0418	12	1.9974	2.7924	19
CBS[c]	1.4632	2.0408	12	1.9972	2.7930	20
BO[d]				1.9972	2.7928	20
"Exact"[e]	1.4633	2.0403	12	1.9977	2.7932	20

[a]Reference 12 (all PESs).
[b]M = 8 PESs of Ref. 31.
[c]Complete basis set limit (present work).
[d]Reference 44.
[e]Exact or best known value. For H_2^+ Ref. 44 (DBOC). For HeH^+ Ref. 3 (experimental fit).

In Table I, we compare the equilibrium distances (R_e), the dissociation energies (D_e) and the number of bound vibrational states (N_v) obtained in the present work (referred as CBS in the following) with those of the PECs used in the previous works[12,31] and with reference values to test the accuracy of the BO approximation. For HeH^+, the reference values reported have been taken from Ref. 3, where a large database of spectroscopic frequencies measured at the μ-Hartree level of accuracy have been fitted to obtain the best "experimental" diatomic curves. In the H_2^+ case, the absence of the dipole moment makes spectroscopic experimental measurements much more difficult. However, its great simplicity from the theoretical point of view has permitted calculations of roto-vibrational states at the highest level of theory[5] beyond the non-relativistic quantum mechanics. Most of these high accuracy calculations, being based on non-BO treatments, do not provide equilibrium bond distances and dissociation energies to compare with the values calculated in the present paper (CBS). Therefore, as reference values for H_2^+ in Table I, we report the parameters obtained in Ref. 44, obtained from BO highly convergent calculations with and without diagonal BO corrections (DBOC). At the number of digits reported in Table I the DBOC curves of Ref. 44 produce the same vibro-rotational frequencies achieved in Ref. 5.

Table I shows that the diatomic curves used in Ref. 12 are about 8 and 15 meV shallower than the CBS PECs for the H_2^+ and the HeH^+ ions, respectively, and support two vibrational bound states less. For RFCI and RMRCI PECs, the discrepancies with the CBS results reduce drastically down to 2 meV. However, in the HeH^+ case the last weakly bound state is still missing in RFCI PEC, although the well is slightly shallower in the CBS calculation. The situation is worse for H_2^+ where the vibrational bound states missing are two for RFCI PEC and one for RMRCI. This is due to the fact that the diatomic functional form used in Ref. 31 does not include the polarization terms of Eq. (4) which is highly relevant to describe the long range part of the diatomic curves. We note that the comparison with the CBS calculations is clearly

better for RMRCI PEC indicating that the extension of the one-electron basis set affects significantly the vibrational dynamics. The comparison between CBS and the reference values shows that the BO approximation changes the dissociation energies within 0.5 meV while the number of vibrational states remains unchanged. Also the differences between the equilibrium distances are small (less than 0.0005 bohr). For H_2^+ the CBS curve reproduces exactly the results of Ref. 44, demonstrating that, within the BO framework, all the digits shown are convergent.

In the Appendix the roto-vibrational frequencies of HeH^+ and H_2^+ are compared with highly accurate theoretical[4,5,45,46] and experimental data.[47] For the PEC used in Ref. 12, only the lowest vibrational levels are at the meV level of accuracy while for the PECs of Ref. 31 the frequencies of all the bound vibrational states, except the weakly bound states very near to the dissociation, reach this level. In particular for these latter PECs, the diatomic curves used in the fit to the MRCI points, using the more extended basis set, show the best comparison with the reference data. The frequencies obtained with the new diatomic curves (CBS results) show that it is possible to obtain a near spectroscopic accuracy for this system also using the BO approximation notwithstanding the relevance of the non-adiabatic effects (and in particular of the DBOC corrections) on the absolute values of the electronic energies, especially when atomic masses are used, as usual in reaction dynamics, to describe the nuclear motion. In fact, the nuclear dynamics is sensitive just to the modifications of the electronic energy with the internuclear distances, so that small changes in the vibrational frequencies are observed when the correction is weakly dependent on the nuclear configurations.

B. The three-body interaction

In Sec. II A, we have shown that significant changes in the dynamics of the diatomic species is observed when an alternative extension of the one-electron basis set is used. In order to quote the accuracy of the *ab initio* energies used in Refs. 12 and 31, it is important to establish whether these changes are larger with respect to the electronic correction coming from triple excitations, neglected in the MRCI treatment of the correlation energies. To understand this crucial point we have performed MRCI calculations on the same set of the internuclear distances of Ref. 31, employing the same Dunning cc-p VQZ basis set used in Full CI calculations. The relative root-mean-square deviation between the energies obtained and the Full CI calculations of Ref. 31 has been found of the order of a few tens of meV. The relative root-mean-square deviation with the MRCI calculations of Refs. 12 and 31 (employing the more extended Dunning cc-p V5Z basis-set) was about two orders of magnitude larger (about 11 meV), indicating that the extension of the one-electron basis set is much more important than the triple excitations included in the Full CI treatment.

III. QUANTUM REACTIVE SCATTERING CALCULATIONS

The potential energy surfaces of Refs. 12 and 31 have been used to calculate integral cross sections (ics) for the scattering of the He atom by the hydrogen molecular ion. Quantum scattering calculations are carried out by a modified and parallelized version of the ABC code.[48] The ABC program employs a time-independent coupled channel hyperspherical coordinate method to calculate the quantum mechanical scattering matrix. The set of coupled hyperradial equations is solved using a logarithmic derivative method.[49] In our modification of the code, an enhanced Numerov propagator[50] is applied to integrate the coupled channel hyperradial equations for all sectors except the last one, where, as in the original code, the logarithmic derivative propagator is used to recover the simplicity of the matching equations. The implementation of this modification has been essential to obtain *S*-matrix elements highly convergent while keeping low the number of sectors. In addition, most of the subroutines have been adapted for parallel implementation in order to optimize the performances of the code (for details of the parallel strategy implemented, see Ref. 51).

The high computational efficiency of the modified and parallelized version of the program has made it possible to calculate total ics convergent within 1% in the full collision energy range from about 2 meV above the reactive threshold up to about 0.3 eV under the threshold of the three-body breakup. At the best of our knowledge, this is the first time that this reaction has been investigated with a time-independent quantum methodology in a so large collision energy range. In the scattering calculations, this large interval has been divided into four subintervals and ten equally spaced energy values have been selected within each subinterval. The input parameters to be used in the ics production runs have been optimized separately for each subinterval. Their numerical values, see Table II, and the related computational requirements markedly change for the intervals considered. The convergence has been tested for all the PESs employed. The results show that there are no relevant differences among

TABLE II. Values of the input parameters used in the calculation of the total integral cross sections. For the definition of the parameters, see text.

Total collision energy[a] (eV)	*Jtotmax*	*kmax*	*emax*[a] (eV)	*jmax*	*drho* (a_0)	*rmax* (a_0)	*dE* (meV)
0.955–0.97	20	20	2.1	24	0.125	30	0.2
0.97–1.17	38	16	2.1	24	0.125	15	1.0
1.17–1.57	54	12	2.3	26	0.125	15	2.0
1.60–2.40	72	12	2.5	28	0.125	15	50.0

[a]Zero energy is in the bottom reactant valley.

the convergence speed of the *S*-matrix elements using different PESs so that the same input parameters (shown in Table II) have been used independently by the PES employed.

As pointed out in other papers[13,16,19] and shown in more detail in Sec. V, in the neighborhood of the reactive threshold the dynamics is strongly dominated by several resonance features. In this energy region, the values of the ics are very sensitive to the number of projections of the total angular momentum (*kmax*), and to obtain the claimed convergence all the allowed values have to be included in the expansion of the wavefunction. This is a consequence of the relevance of the Coriolis coupling for this reaction and its isotopic variants[14,18] and of its role in the breakup mechanism of the resonance complex.[52] Accordingly, in this case the use of coupled state approximations for the description of the dynamics is not recommended.[12,52] In order to completely resolve the narrow resonance structures appearing in the ics a fine energy grid (*dE*) had to be used in the production runs. At higher total energy (above 1.5 eV), the ics energy profile becomes smoother. The number of partial waves to be propagated (*Jtotmax*) is very high (≈70), but the convergence on *kmax* is faster than in the low collision energy range, so leading to a drastic reduction of the number of the coupled hyperradial equations. We comment that this unexpected behavior is very different from that we have found in other systems (see, e.g., Refs. 51 and 53), where typically the value of *kmax* increases with the collision energy. It is again due to the lower relevance of the resonance mechanism at higher energies that increases the classical character of the reactive collisions.[30]

The convergence of the cut-off parameter *emax* (the energy of the most excited roto-vibrational level included into the basis set) is particularly important, being this parameter strictly related to the dimension of the asymptotic basis set employed. In the energy range considered in this paper, convergent ics have been obtained with the values reported in Table II. However, if *emax* is set at a value close to the energy of the triatomic breakup (see Table I), the ics differ markedly from their convergency values. This is due to the poor convergence of the weakly bound roto-vibrational states of the reactant and product molecules lying close to the dissociation threshold. When the rotational levels of the two last bound vibrational states nearest to the threshold are included into the asymptotic basis set, the calculation fails because the maximum elongation of the diatomic species permitted by the code is not sufficient to give convergent roto-vibrational levels. For the title reaction, this problem arises when *emax* is very near to the dissociation limit (around to 2.7 eV) and this, of course, limits the collision energy interval that can be investigated with the ABC code. However, the limitation is not so serious because, at the best of our knowledge, close coupling time-independent quantum reactive scattering calculations above the energy corresponding to the triatomic break up (around to 2.78 eV) are intrinsically not permitted in any available algorithm because of the difficulty to properly describe quantum mechanically the collision induced dissociation dynamics (for a recent wave-packet couple state study of the HeH_2^+ system see Ref. 54). In this paper, we limit our calculations to the maximum total energy of 2.4 eV, where the accuracy of the calculation can still be checked with sufficient reliability.

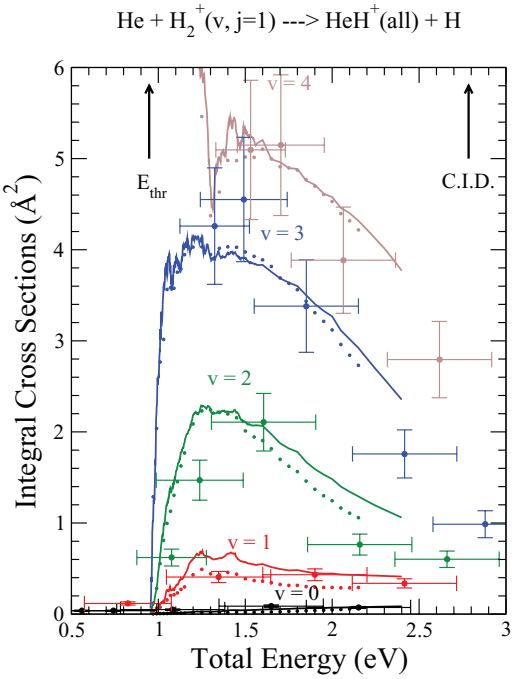

FIG. 1. Total ics for the reaction He + $H_2^+(v = 0–4, j = 1) \rightarrow HeH^+ +$ H as a function of the total (translational + rotational + vibrational including the zero point) energy. Solid lines and filled circles are quantum mechanical results obtained using PM10 and RMRCI PESs, respectively. The experimental results (filled circles with error bars) have been taken from Ref. 56, normalized by a common scaling factor to optimize the agreement with the theoretical results. The error bars reported for the energy are taken from Ref. 57 while the error bars for the ics (not reported in the original work) are estimated by us to be around 30%. The arrows in the plot indicate the reactive threshold (E_{thr}) and the three-body breakup energies.

Also we note that the values of *jmax* employed, see Table II, are close to the maximum value of the rotational angular momentum quantum number imposed by the *emax* parameter. So the reduction due to this cutoff parameter is negligible for this reaction. This is an indication of a large rotational energy transfer taking place during the reactive collisions.

IV. COMPARISON WITH THE EXPERIMENTS

As reported in Sec. I, most of the state-of-the-art reaction dynamics calculations for the He + H_2^+ reaction[12,16,19] have been performed with PM12 PES. Unfortunately, as reported in Sec. II, this fitting does not respect strictly the exchange symmetry of the hydrogen atoms (see Sec. II) and therefore is not the most appropriated for benchmark calculations of reaction dynamics. For this reason, to test the accuracy of the PESs of Ref. 12 we have performed extensive scattering calculations, with the input parameters given in Table II, with PM10 fit. A total number of 492 energies have been run for each diatomic parity of the hydrogen molecular ion for this PES. Calculations for a coarse-grained energy grid (about 30 energies) have been also performed with RMRCI and RFCI PESs of Ref. 31 to compare the reaction dynamics results with the experimental data. A FORTRAN subroutine of PM10 and RMRCI PESs and the ics shown in this section for $H_2^+(v, j = 1)$ are given in the supplementary material[55] for benchmark purposes.

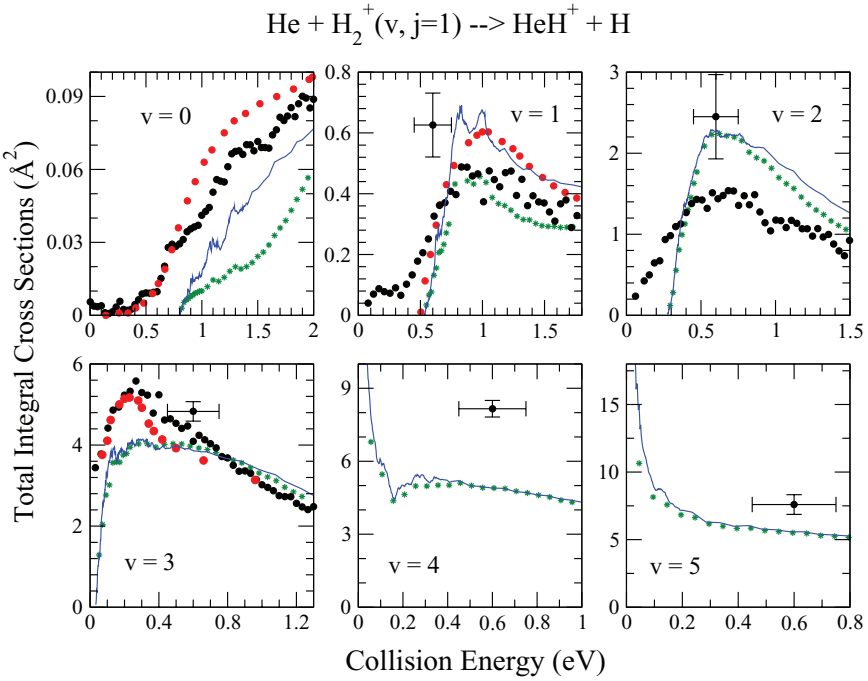

FIG. 2. Comparison among theoretical total ics for the reaction He + $H_2^+(v = 0–5, j = 1) \rightarrow HeH^+ + H$ as a function of the translational collision energy and experimental results (absolute values). Each panel corresponds to a different initial vibrational states v as indicated. Solid blue lines refer to calculations performed with PM10 PES. Green stars symbols correspond to calculations at specific energies, performed with RMRCI PES. Red filled circles are the experiments of Ref. 29. Filled black circles with and without error bars are the FPI-PESICO and the autoionization resonances results of Ref. 30, respectively (see text for details).

In Fig. 1, total ics for the *ortho*-hydrogen molecular ion in its ground rotational state ($j = 1$) and for the vibrational states $v = 0$–4 are compared with the experimental measurements.[56] Being the experimental values in relative units, in Fig. 1 they have been normalized by a common scaling factor to optimize the agreement with the theoretical data. Following Ref. 56 the ics are shown as a function of the total energy. The ics for $v = 1$–3 increase rapidly in the neighborhood of the reactive threshold and then decline slowly. The maximum is more pronounced for high vibrational initial states and the vibrational energy strongly enhances the reactivity of the H_2^+. This behavior, known since the early experimental studies,[29] is very well reproduced by the calculations. The integral cross section corresponding to the exothermic $v = 4$ channel behaves differently: it increases indefinitely at the lowest translational energies and exhibits a minimum followed by a maximum as the energy increases. We note that this peculiar behavior, see also Ref. 16, was not expected from the experiments[56] where the higher collision energy measurements were extrapolated to zero. From the comparison we can conclude that the theoretical calculations reproduce sufficiently well the experimental data. Many narrow resonance features are present up to the maxima of the excitation functions especially for the higher vibrational states, while a smoother behavior is shown at higher total energies. The comparison shown in Fig. 1 between the calculations using PM10 and RMRCI PESs indicates that the global behavior of the total ics is not very sensitive to the PES used with differences, for most of the reactants vibrational states, within the estimated error bars of the experiment. Notwithstanding the better description of the diatomic interaction (see Sec. II A and the Appendix) there are not substantial improvements in using MRCI, although a slightly better agreement with the experiments can be noted in the high total energy range.

In Fig. 2, the total ics for $v = 0$–5 and $j = 1$ are compared with the experiments of Refs. 29 and 30. In Ref. 30 two different sets of results were supplied. The first set concerns ics for the reactants vibrational levels $v = 0$–3 measured as a function of the translational collision energy, using high-resolution vacuum ultraviolet to prepare reactant ions through excitation of autoionization resonances. In the second set, roto-vibrational selected reactant ions were obtained using pulsed-field-ionization-photoelectron-secondary ion coincidence (FPI-PESICO) approach and the ics were measured at two collision energies (0.6 and 3.1 eV) for most of the bound and quasi-bound vibrational states of H_2^+. The higher energy is above the three-body breakup and cannot be probed by our quantum mechanical calculations (see Sec. III). The first set and the first energy of the second set are reported in Fig. 2 as black circles without and with error bars, respectively, while the red circles are the experimental values of Refs. 29 and 58 calibrated according to previous theoretical models.[24,59] In this case, the experimental ics are absolute values. Also, we have performed some calculations with PM12 PES and tested the relevance on the dynamics of the unphysical asymmetry of the PES. The results are supplied in the supplementary material[55] together with an explicit comparison with previous wave packets[16,19] and time independent hyperquantization algorithm[25] results.[12]

The comparison of the ics calculated using PM10 and RMRCI PESs with the experimental results in Fig. 2 shows an

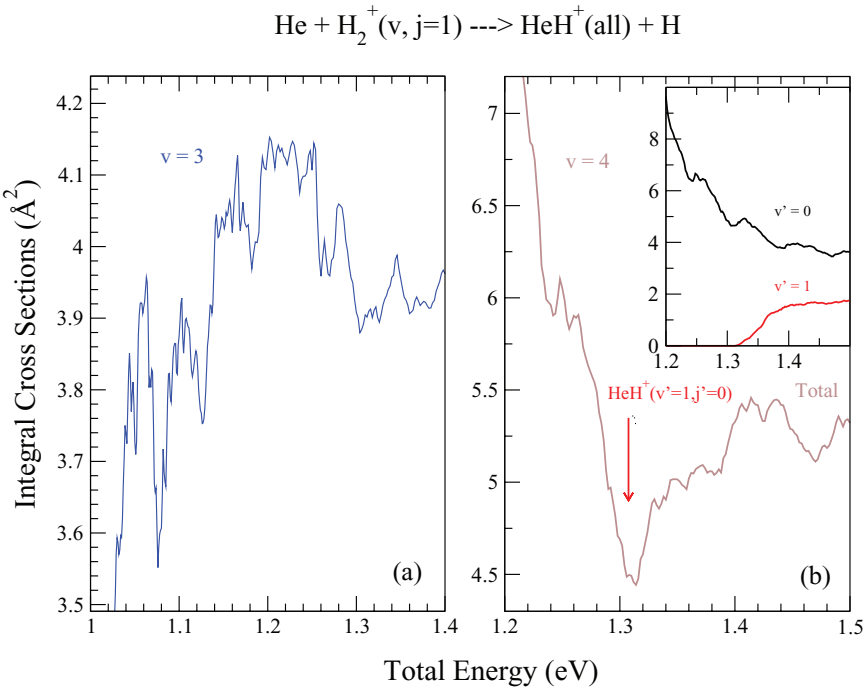

FIG. 3. Blow-up of Fig. 1 at the energy near to the maximum of $v = 3$ (a) and to the minimum of $v = 4$ (b) to show the details of the resonance features. Total ics as a function of the total collision energy are quantum mechanical results obtained using PM10 PES. The arrow in (b) shows the energy threshold of the $HeH^+(v' = 1)$ channel. The inset reports the energy behaviors of the vibrational resolved integral cross sections for the $He + H_2^+(v = 4, j = 1)$ reaction.

overall good agreement but with relevant differences between the two sets of theoretical data. We will analyze later the differences between the results obtained with the two PESs. The presence of considerable signal below the energy thresholds for the lower reactants vibrational states is an artifact of the measurements, probably due to the low rotational and translational resolutions and/or to possible contamination of the product of higher vibrational states.[30] To account for the translational resolution, Ref. 30 also reports deconvoluted ics obtained fitting the experimental data with a modified line-of-centers functional form[60] that eliminates the unphysical behaviors. However, we prefer to compare directly with the measurements, kindly available by the authors, avoiding to introduce an additional source of errors coming from the simple dynamical model used to fit the data. For $v = 0$ and 1, the results using PM10 PES show a global better agreement with respect to RMRCI PES. The agreement of the $v = 1$ results with the experiment of Ref. 29 and of the $v = 2$ with the FPI-PESICO experiment of Ref. 30 is impressive. For higher vibrational states and in particular for $v = 4$, the agreement with the FPI-PESICO results is much lower. We note that this is in contradiction with the experimental results of Fig. 1 where a much lower vibrational ratio was found for $v = 4$ in agreement with the theoretical data. Also for $v = 3$ the ics maximum is flatter and appears at higher collision energies than that of the experiments.

V. ANALYSIS OF THE RESULTS

As mentioned in Secs. I–IV, the resonance phenomenon plays a relevant role in the description of the dynamics of the title reaction. To better show the details of the resonance pattern in Fig. 3 the theoretical ics in the regions of the maximum for $v = 3$ and of the minimum for $v = 4$ of Fig. 2 are reported in a narrower energy range. As shown elsewhere,[16,19] the maximum in the ics arises from the superposition of several narrow resonance peaks in the reaction probabilities. The sum over the total angular momentum quantum number smears out most resonance patterns but as shown in Fig. 3(a) significant features survive. From the width of the peak it is evident that the features come from Feshbach resonances due to trapping in quasi-bound and virtual states, arguably supported by the main deep well of the reaction in the collinear configuration.[12] However, the analysis in Ref. 12 has shown that another local well (unstable with respect to the entrance channel) exists in the insertion collinear configuration with the He atom in the middle between the two protons. Intra-molecular dynamics between metastable states supported by the two wells could play an important role in enhancing the resonance dynamics.[61] The role of the insertion mechanism can also be inferred by the strong sensitivity to *kmax* (see Sec. III) of the resonance pattern. More detailed analysis, as reported in Refs. 62 and 63 including also studies of differential cross sections,[64] is required to understand this complex resonance behavior. Convolution of the resonance peaks gives the global maxima shown in Fig. 1 for $v = 1$–3. The global behavior of the ics is typical of reactions with an energy barrier (see Ref. 65 and in particular Fig. 3.8 and problem L), where the barrier is the endothermicity of the reaction. Completely different is the behavior of the $v = 4$ exothermic reaction that shows a typical low energy behavior of reactions with no energy threshold. In the simplest capture model for ion molecule reaction a divergent threshold behavior is predicted with the ics decreasing with the collision

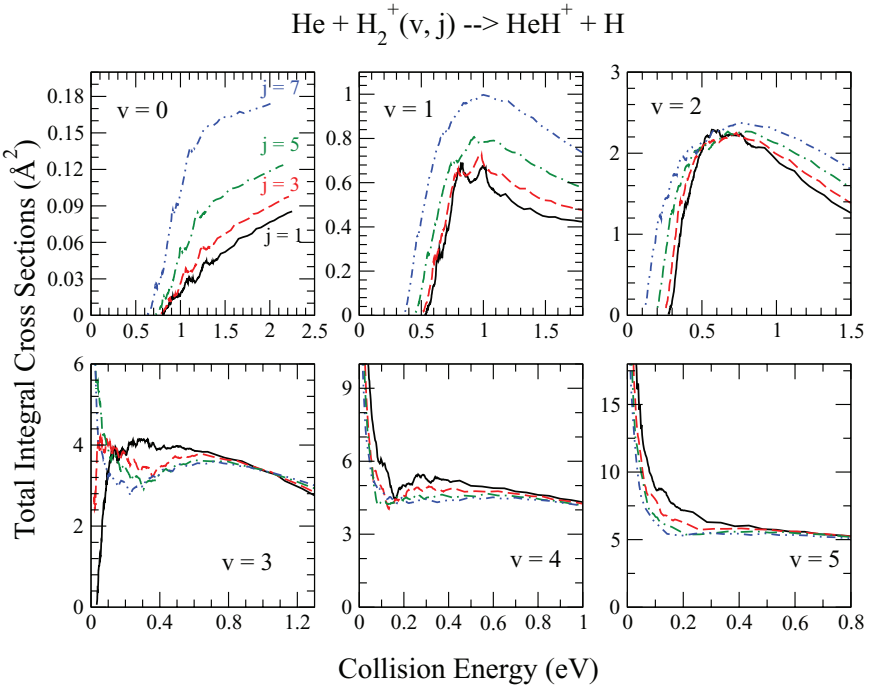

FIG. 4. Total ics for the reaction He + H_2^+(v= 0–5, j=1, 3, 5, and 7) → HeH^+ + H as a function of the translational collision energy. Each panel corresponds to a different initial vibrational states v as indicated. The calculations reported are obtained using PM10 PES. Different lines and colors refer to different initial rotational states: black solid j= 1, red dashed j = 3, green dot-dashed j = 5, and blue dot-dot-dashed j= 7.

energy as $E_{coll}^{-1/2}$.[65] However, we can note that the behavior of the $v = 4$ total ics (magnified in Fig. 3(b)) is more complex showing a narrow minimum as a function of the collision energy. The inset in Fig. 3(b) shows that this feature arises from the opening of the $HeH^+(v = 1)$ channel where the minimum is located. The vibrational deconvolution of the total ics reported in the inset shows that the minimum is given by the sum of two opposite behaviors: the $v = 0$ behavior, typical of reactions without threshold, and of the ics of $v = 1$ that exhibits the post-threshold character predicted by the line-of-centers model.[65] Also, signatures of a broad resonance appear in the $v' = 0$ ics at the opening of the $v' = 1$ channel.

The differences between FPI-PESICO and autoionization resonances results (where available), as well as some of the discrepancies between theoretical and experimental data, could be explained taking into account of the influence of the rotational energy. To analyze this aspect, in Fig. 4 we report the ics obtained with PM10 PES, for different initial rotational states (j = 1–7) of the *ortho*-H_2^+. Interesting information can be extracted from the analysis of the figure. For low v there is a strong rotational effect on the reactivity with the ics for $j = 7$ several times larger than the ics of the ground rotational state. The effect decreases for higher vibrational states and changes sign for v larger than 3, so that the reactivity becomes lower for high j except near to the threshold. In most of the cases there is also an interesting change of the ics behavior with the initial rotational energy. For $v = 0$ the reactivity of the high j sharply increases at the threshold and becomes nearly constant at higher collision energies. For $v = 1$ and 2 the ics maximum of the higher j is broader and slightly shifted at higher collision energies. For $v = 3$ in the $j = 3$ case the maximum shifts toward lower collision energies and a broad minimum appears. The minimum shifts at lower energies with the increasing of the rotational state and from $j = 5$ the maximum disappears and the ics start to increase at the threshold. The fast change in the ics threshold behavior with the rotational energy for $v = 3$, clearly shows that this behavior is completely dependent from the energetics of the reaction. In fact, the $v = 3$ and j= 5 roto-vibrational level is the first exothermic channel of the reactants so that beginning from this reactive channel the ics exhibit the behavior predicted by the capture model (see discussion of Fig. 3(b)). For higher v, the rotational effect is lower especially for higher j. The ics decrease rapidly at low collision energy and become nearly constant for high values of j at collision energy above 200 meV. Regarding resonances, we can note that, as in the F+HD system,[66] the most important features arise for the lower rotational states while for higher j the ics are smoother and with a less structured pattern.

The role of the rotational excitation could explain most of the discrepancies among the experimental results shown in Fig. 2. In fact, rotational purity of the reactants is difficult to be obtained in this kind of experiments.[30] The only data claimed to have rotational resolution in the reactant ion are the FPI-PESICO experiments of Ref. 30, while for the other experiments the rotational distribution of the reactants is generally unknown and hardly to be simulated. This makes more complicated the evaluation of the quality of the PESs, considering that for the first vibrational states the theoretical results are more sensitive to the internuclear interaction. However, we can note that the rotational impurity of the beam could explain the differences among theoretical and experimental excitation functions of the first four vibrational states but not the differences with the FPI-PESICO measurements

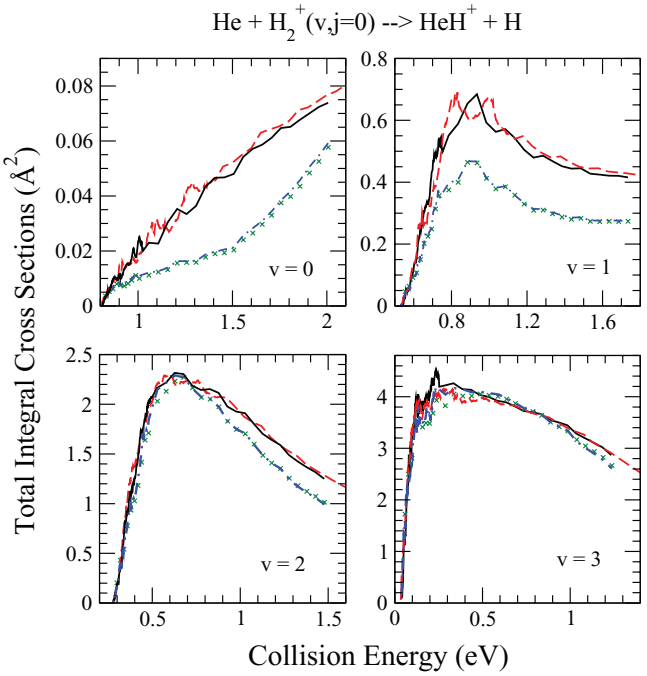

FIG. 5. Total ics for the reaction He + $H_2^+(v = 0–3, j= 0) \rightarrow HeH^+ + H$ as a function of the translational collision energy. Each panel corresponds to a different initial vibrational states v as indicated. Solid black, blue dotted curves and X crosses symbols are the quantum mechanical results obtained using PM10, RMRCI, and RFCI PESs, respectively. To show differences between the ground states reactivity of the *ortho*- and *para*-H_2^+, the j= 1 results of Fig. 4 are also reported as red dashed lines.

for the higher vibrational states, which are underestimated by the theory, especially in the $v = 4$ case, with all the PESs used and with the rotational excitation that decrease the reactivity. The stability with the PES of the $v = 4$ ics and the disagreement with the experiment[56] (see Fig. 1), suggest that probably additional experimental work is required to confirm the reliability of the experimental data at least regarding this particular reactive channel. Moreover, because the reactive thresholds significantly shift with the reactant rotational energy (see Fig. 4), the lack of rotational resolution can partially account for the unphysical under-threshold behavior found in the first set of experiments of Ref. 30 especially if high H_2^+ rotational states were populated by the excitation of the autoionization resonances.

The important rotational enhancement shown in Fig. 4 could cast doubts on aspects of the previous theoretical investigations performed almost exclusively with *para*-H_2^+ in its ground rotational state. To check this, in Fig. 5 we compare *ortho*- and *para*-H_2^+ ics for v =0–3 obtained with PM10 PES. The overall behavior of the excitation functions is very similar for the two reactants so that differences between curves can just be barely seen at the scale of Fig. 5. However, significant differences between the resonance patterns exist especially for $v = 1$, where two significant maxima in place of one are reported in the *ortho*- case. This is due to the large reactant character of the three-body complex localized in the deep triatomic well near to the reactants valley.[12] Figure 5 also compares the ics of the ground rotational state of the *para*-H_2^+ obtained with RMRCI and RFCI PESs. No differences appear at the scale of the plots, in spite of the significant differences between the energies of the *ab initio* points (see Sec. II B). Nevertheless, the differences between the PESs of Refs. 12 and 31 are remarkable especially for the first two vibrational states, also considering that for the RMRCI case there are no differences between the quality of the *ab initio* energies (see Sec. II). Because reaction dynamics results are of course sensitive to the global PES used it is difficult to establish if these differences come from the better diatomic curves used in the RMRCI PES or from the additional repulsive energies fitted in Ref. 12. However, in Sec. II and in the Appendix we have shown that the larger differences in the diatomic curves are for higher vibrational states so that if the origin of the discrepancies should come from the diatomic curves the larger differences should be observed for high v. For low v values where the differences occur, the higher translational energy of the reactants can probe more likely the repulsive region of the PES where the PESs most differ. This result suggests that to improve the accuracy of the PES it is likely more important to enlarge the number of the *ab initio* points (especially in the repulsive region) rather than to increase their accuracy.

In Ref. 12, it is suggested that a sensitive test of the accuracy of the PES could be given by the ics behavior at collision energies close to the reactivity threshold where the ics increase rapidly and significant resonance structures are observed, especially for the $v = 3$ reaction. These features have attracted a wide interest in the literature (see, e.g., Refs. 67–69). In Fig. 6, we compare in different plots

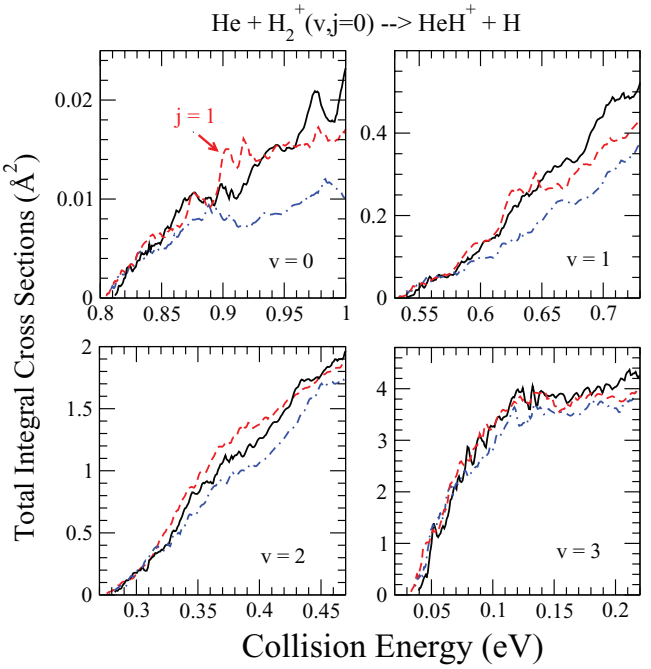

FIG. 6. Comparison of the resonance energy patterns for the ground rotational states of the *para*- (black solid lines) and *ortho*- (red dashed) reactions $He + H_2^+(v = 0–3) \rightarrow HeH^+ + H$ in the near threshold collision energy range (2–200 meV). Each panel corresponds to a different initial vibrational states v, as indicated. The reported calculations are performed with PM10 PES. To compare with the *para*- results, $j = 0$ ics calculated with RMRCI PES are also reported as blue dot-dashed lines. A fine energy grid of 0.1 meV has been used to resolve the resonance energy patterns.

the ics v =0–3 behavior as a function of the translational collision energies for the ground rotational states of the *ortho*- and *para*-H_2^+ obtained with PM10 and RMRCI PESs. To converge the resonance features full helicity calculations ($Jmax = kmax = 20$) were performed in the energy range reported. The post-threshold region is dominated by strong resonance features especially for $v = 0$ and 3. However, to establish quantitatively the extent of the resonance mechanism contribution to the reactivity, a deeper analysis as the one presented in Ref. 70 should be done to separate the resonances contribution from the other direct mechanisms[69] acting on the reaction. The resonance behavior appears as a fine detail of the excitation functions and is very sensitive to the *ortho*- or *para*-parity of the diatom and to the details of the PES employed and in particular to the accuracy of the well. Quasi-bound and virtual states responsible of the Feshbach resonances formation are in fact very sensitive to the detail of the potential well and likely potential energy surfaces with near spectroscopic accuracy are required to define these resonance features. However, such effects are probably too small and too narrow for being detected in molecular beam experiments, at least with the energy resolutions presently available. Nevertheless, important recent advances[71] in the control of the kinetic ion energy in cold and ultra-cold conditions make well hope to reach the resolution required to investigate the rich resonance dynamics of this and other ionic systems.

VI. CONCLUSIONS AND PERSPECTIVES

In this article we have revised (see Sec. II) several aspects of previous *ab initio* studies[12,31] of the interaction of the HeH_2^+ system, in order to assess the accuracies of the global PESs achieved in that works. A detailed comparison of the spectroscopic properties of the diatomic species (see Sec. II A and also the Appendix) shows that the diatomic curves[23] used to build up the PESs of Ref. 12 present some previously overlooked inaccuracies, more relevant for the higher vibrational states. Agreement with the reference data is much more satisfactory for the diatomic potentials of Ref. 31 especially for those used in the fit to the MRCI points employing a more extended basis set.

To estimate the accuracy of the three-body term of the PES is a difficult task. As discussed in the Introduction, several sources of errors must be taken into account and the analysis cannot be limited to the comparison of the root-mean-square deviations. To assess the quality of the *ab initio* data, it is important to establish whether the error introduced by the MRCI treatment for the calculation of the correlation energy is larger than the error introduced by the truncation of the basis set. The direct comparison of the *ab initio* energies (Sec. II B) shows that this error is about two order of magnitude less demonstrating that the set of *ab initio* energies used in the MRCI fit of Ref. 31 is more accurate than the Full CI one. In order to establish the accuracy of the PESs in regions of the configuration space not covered by the *ab initio* calculations, reaction dynamics calculations are needed. Within the time-independent approach to quantum reaction dynamics (Sec. III), highly convergent total integral cross sections for the scattering of the helium atom from the hydrogen molecular ion in a selected quantum state (v = 0–5, and j = 0–7) have been obtained for the first time over a wide energy range, where several experimental data[29,30,56] are available.

The theoretical results reproduce reasonably well the global behavior of the experiment of Ref. 56 (see Fig. 1), while less satisfactory is the comparison with the experiments of Ref. 30 (Fig. 2) especially regarding the few measurements for $v = 4$ and 5 where much higher vibrational ratios were observed. The insensitivity to the ratio with the PESs employed and the disagreement with the previous experimental data[56] shows that more experimental work is required to clarify the origin of the discrepancies. The dynamics is not very sensitive, at the scale of the experiments, to the differences among the PESs employed, so that these differences are in most cases within the accuracy of the experimental data. Only when H_2^+ is in the ground and first excited vibrational levels (see Fig. 2), these differences are able to change the quality of the comparison with the experiments. For these low vibrational states, a strong rotational enhancement of the reaction yields is shown in Fig. 4 casting doubts about the reliability of the comparison with the experimental data. In fact, little information is available in the literature about the rotational distributions of the reactants molecular ion beams and experimental difficulties make hard to obtain experiments with high rotational resolution for most systems, including this one.[30]

Nevertheless, the relevant differences between the ics obtained with PM10 and RMRCI PESs (see Fig. 2) and the close agreement of the results obtained with RFCI and RMRCI PESs (Fig. 5), could give important information on the sensitivity of the reaction dynamics to the description of the interaction. In fact, it is hard to believe that these differences come from the higher accuracy of the diatomic curves used in the RMRCI and RFCI PESs because larger differences should be found in the dynamics of the higher vibrational states where the larger differences among the diatomic curves appear. More likely the differences come from the three-body repulsive region probed by the higher collision energy collisions of the lowest vibrational states, where no *ab initio* points were employed in the fit of the PESs of Ref. 31 (see Sec. II). This small number of internuclear geometries could be highly relevant to the reaction dynamics in order to establish the exact position of the classical turning points. Nevertheless a final answer with respect to the real accuracy of the PESs employed can be only given by comparison with a PES of an higher level of accuracy. The results obtained indicate that to improve the comparison with the experimental data it is likely more important to cover a more extended range of internuclear geometries, especially in the repulsive region of the PES rather than to increase the quality of the *ab initio* energies.

Additionally, at small translational collision energies the details of the resonance pattern (Fig. 6) are very sensitive to the accuracy of the PES used. Pronounced resonance features appear especially for the $v = 0$ and $v = 3$ reactions. To obtain realistic ics in the neighborhood of the reactive thresholds, a high accuracy of the PES is required. On this aspect, we have shown in the Appendix that *ab initio* energies obtained with the CBS limit are able to reach a near spectroscopic accuracy for this system also remaining within the BO framework. This

is possible because the main source of non-adiabatic effects for this system comes from the diagonal BO corrections that are weakly dependent on the internuclear distances.

In summary, this work indicates how for this and similar systems a global PES at a near spectroscopic level of accuracy is currently within reach. To achieve such a high accuracy, a fitting functional form (see Sec. II and Appendix) providing a good description of the long-range interaction (highly relevant for the dynamics of charged systems) is required. The improvements in both the accuracy of the PES and in the quantum reactive scattering code presented also in this paper (see Sec. III) will permit to supply realistic results also at cold and ultra-cold temperatures that are relevant in the astrochemical applications of this system and its isotopic variants. The strong roto-vibrational enhancement observed for this reaction (see Fig. 4) could have important consequence in the chemical network of the early universe evolution.

ACKNOWLEDGMENTS

The authors thank Dr. X. Tang and Professor C.-Y. Ng (Davis) for supplying their experimental data and for discussions. A particular acknowledgment is addressed to Professor M. Paniagua (Madrid) for scientific discussions and encouragements. We are also grateful to Dr. T. Gonzalez-Lezana (Madrid) for supplying subroutines codes and Dr. F. Colavecchia (Bariloche) for discussions. The work has been performed under the HPC-EUROPA2 project (Project No.: 228398) with the support of the European Commission - Capacities Area - Research Infrastructures. D.D.F., V.A., and S.C. thank also the Italian MIUR for PRIN contracts. A.A. acknowledges support by the program CONSOLIDER-INGENIO of Ministerio de Economia y Competitividad (Spain) under Grant No. CSD2009-00038, entitled "Molecular Astrophysics: the Herschel and Alma Era," Grant No. FIS2011-29596-C02-02, and by Comunidad Autonoma de Madrid (CAM) under Grant No. S-2009/MAT/1467.

APPENDIX: DETAILED COMPARISON OF THE DIATOMIC VIBRO-ROTATIONAL FREQUENCIES: MASS AND NON-BO EFFECTS FOR HeH^+ AND H_2^+

Detailed comparison of vibrational frequencies are sensitive to the exact values used for the nuclear masses. Many results in the literature (see, e.g., Refs. 72 and 73) have shown that, at least for the H_2^+ and H_3^+ ions, using atomic masses in place to the nuclear ones or combination between them,[74] led to higher accuracy for vibrational frequencies, partially balancing non-adiabatic effects in the vibrational dynamics. In fact, diagonal BO corrections, highly relevant in these light molecules, include effects coming from the separation of the center of mass of the system,[75] that introduces terms in the nuclear Hamiltonian of the order of the ratio between the electron and the nuclear masses (neglected in the BO approximation). These terms are partially accounted for in the vibrational dynamics by retaining the electron mass into the nuclear one.[72]

In Table III we report the vibrational frequencies ($E(v, j = 0) - E(v-1, j = 0)$) for all the bound states of the H_2^+. The first five columns list results obtained using nuclear masses,[76] strictly following the BO framework upon which our calculations have been based. In order to compare with the reference data,[5] in the sixth column we also report the values obtained with the complete basis set using atomic masses (CBS a.m.) data. From the comparison with the CBS results, we can observe that the PEC used in Ref. 12 reproduces satisfactorily the frequencies at the meV level only for the ground and the first vibrational states, while the differences for the highest supported vibrational state are of the order of ≈10 meV. For the RMRCI PEC the meV accuracy is preserved until $v = 9$, while for the RFCI case until $v = 5$. However, for these last two PECs, the differences are confined within 2 meV except for the frequency of the highest vibrationally excited bound state, where the differences are of the order of 4–5 meV. Comparison with the BO calculations in Ref. 45 (also using nuclear masses) shows that all the digits reported for the CBS calculations are convergent at the BO level. As "Exact" results we report the calculations of Ref. 5 including non-adiabatic, relativistic, and quantum electron dynamics effects. Since relativistic and quantum field corrections to the quantum theory do not affect the digits shown in Table III, the discrepancies with the CBS results are essentially to be attributed to the BO approximation. We can see that these differences are within 1–2 wavenumbers for all the bound vibrational states of the system. The use of atomic in place of nuclear masses ameliorates the agreement for all the vibrational states, as analyzed by the previously cited papers.[72,73]

TABLE III. Vibrational frequencies ($E(v, j = 0) - E(v-1, j = 0)$) in cm^{-1} of the bound vibrational states of H_2^+ for different diatomic curves.

v	PM[a]	RFCI[b]	RMRCI[b]	CBS[c]	BO[d]	CBS a.m.[c]	"Exact"[e]
Z.P.E.[f]	1153.3	1150.0	1149.4	1149.8		1149.5	
1	2197.1	2194.5	2192.4	2192.1	2192.0	2191.5	2191.1
2	2075.1	2068.1	2066.0	2064.7	2064.7	2064.2	2063.9
3	1959.3	1945.3	1943.1	1941.5	1941.6	1941.1	1940.9
4	1847.0	1827.0	1823.7	1822.0	1822.0	1821.6	1821.5
5	1736.2	1712.8	1707.6	1705.4	1705.4	1705.1	1705.0
6	1625.5	1601.8	1594.4	1591.1	1591.1	1590.9	1590.8
7	1513.9	1492.4	1483.4	1478.4	1478.4	1478.2	1478.2
8	1400.6	1383.4	1373.6	1366.8	1366.8	1366.6	1366.7
9	1285.0	1273.4	1264.0	1255.5	1255.4	1255.4	1255.5
10	1166.5	1161.4	1153.5	1143.8	1143.7	1143.8	1143.9
11	1044.7	1046.4	1041.1	1031.0	1030.8	1031.0	1031.1
12	918.9	927.6	925.7	916.2	915.9	916.3	916.3
13	788.4	804.1	806.3	798.4	798.1	798.7	798.7
14	652.4	675.1	681.6	676.7	676.3	676.9	677.0
15	509.8	539.3	550.4	549.6	549.1	549.9	550.1
16	358.8	395.4	410.9	415.9	415.8	416.4	416.8
17	196.1	241.0	260.6	274.9	275.0	275.5	276.2
18			94.4	130.0	130.0	130.7	131.6
19				22.5	22.7	22.8	23.3

[a]Reference 12 (all PESs).
[b]M = 8 PESs of Ref. 31.
[c]Complete basis set limit (present work). In the column a.m. atomic masses were employed.
[d]Reference 45.
[e]Exact or best known value (Ref. 5).
[f]Zero point Energy.

TABLE IV. Vibrational frequencies ($E(v, j=0)-E(v-1, j=0)$) in cm^{-1} of the bound vibrational states of HeH^+ for different diatomic curves.

v	PM[a]	RFCI[b]	RMRCI[b]	CBS[c]	CBS a.m.[c]	"Exact"[d]
Z.P.E.[e]	1517.5	1577.2	1573.8	1575.2	1574.8	
1	2910.2	2915.3	2911.3	2912.6	2911.9	2911.0
2	2608.1	2607.7	2606.7	2605.4	2604.9	2604.2
3	2304.1	2300.3	2298.8	2296.7	2296.4	2295.6
4	1995.5	1988.6	1985.2	1983.2	1983.0	1982.1
5	1679.8	1668.7	1663.7	1661.4	1661.4	1660.4
6	1353.7	1338.7	1333.0	1328.9	1329.0	1327.9
7	1013.3	1000.7	992.8	985.6	985.9	984.4
8	654.7	660.3	649.0	640.3	640.8	639.3
9	283.1	327.4	334.4	328.6	329.1	327.4
10		87.5	114.0	116.7	117.0	116.2
11			5.5	24.7	24.8	24.4

[a]Reference 12 (all PESs).
[b]M = 8 PESs of Ref. 31.
[c]Complete basis set limit (present work). In the column a.m. atomic masses were employed.
[d]Exact or best known value (Refs. 4 and 46).
[e]Zero point energy.

In Table IV we report the vibrational frequencies for the bound states of the hydrohelium cation. Labeled as "Exact" values, we report the results of Refs. 4 and 46 including non-adiabatic and relativistic effects. From the comparison with the CBS data, we can observe that the PEC used in Ref. 12 produces vibrational frequencies accurate to within about 1 meV for the lowest three vibrational states, but increasing the vibrational quantum number the agreement deteriorates up to differences of about 5 meV for the highest vibrational state supported by this PEC. Again, the agreement is much better for the PECs of Ref. 31 where all the vibrational frequencies, except the last weakly bound state, are within 1 meV for RMRCI PEC. The results are slightly worse for RFCI PEC especially for high vibrational numbers, where the differences in the vibrational energies are of 2–3 meV. The comparison with the reference results,[4,46] shows that also for this case our diatomic CBS curve produce vibrational frequencies with nearly absolute spectroscopic accuracy, with differences within one wavenumber for all the vibrational frequencies supported by the system. However, in this case, differently from H_2^+, we do not observe a clear improvement by the use of atomic masses. In fact, a better agreement is only observed for $v < 7$, while results deteriorate for larger v, where the correction obtained increasing the masses changes sign.

Similar considerations can be applied to excited rotational states comparing frequencies with those available from theoretical and/or experimental studies. In the HeH^+ case it is also possible a direct comparison with the spectroscopic data. As an example, the comparison with some experimental pure rotational transitions obtained by Liu and Davies[47] at the μ-Hartree level of accuracy is shown in Table V. Note that, although the absolute accuracy of the frequencies is higher, the relative differences are similar to those of the vibrational frequencies of Tables III and IV.

TABLE V. Pure rotational transitions ($E(v, j+1)-E(v, j)$) in cm^{-1} of the ground, first, and second excited vibrational states of HeH^+ for different diatomic curves.

j	PM[a]	RFCI[b]	RMRCI[b]	CBS[c]	CBS a.m.[c]	Experiment[d]
				$v=0$		
13	780.36	778.43	778.37	778.60	778.30	778.22
14	812.75	810.99	810.89	811.10	810.80	810.71
15	840.95	839.38	839.24	839.41	839.12	839.01
16	864.80	863.45	863.26	863.41	863.11	862.98
17	884.17	883.06	882.81	882.91	882.63	882.48
18	898.90	898.02	897.64	897.76	897.50	897.33
				$v=1$		
13	706.83	704.55	704.81	704.60	704.35	704.27
14	734.08	731.84	732.03	731.76	731.52	731.43
15	756.98	754.80	754.90	754.59	754.35	754.23
16	775.29	773.23	773.18	772.82	772.60	772.46
17	778.80	786.83	786.62	786.20	786.00	785.84
18	797.16	795.30	794.84	794.38	794.20	794.00
				$v=2$		
13	630.60	628.08	627.96	627.63	627.44	627.32
14	651.91	649.29	649.02	648.64	648.46	648.32
15	668.50	665.79	665.30	664.88	664.73	664.56
16	679.99	677.15	676.42	675.95	675.80	675.61
17	685.86	682.83	681.78	681.25	681.14	680.90
18	685.35	682.05	680.61	679.94	679.89	679.59

[a]Reference 12 (all PESs).
[b]M = 8 PESs of Ref. 31.
[c]Complete basis set limit (present work). In the column a.m. atomic masses were employed.
[d]Reference 47.

[1]M. Rosi, P. Candori, S. Falcinelli, M. S. P. Mundim, F. Pirani, and F. Vecchiocattivi, Lect. Notes Comput. Sci. **7333**, 316 (2012).
[2]V. Aquilanti, K. C. Mundim, S. Cavalli, D. De Fazio, A. Aguilar, and J. M. Lucas, Chem. Phys. **398**, 186 (2012).
[3]J. A. Coxon and P. G. Hajigeorgiou, J. Mol. Spectrosc. **193**, 306 (1999).
[4]M. Stanke, D. Kedziera, M. Molski, S. Bubin, M. Barysz, and L. Adamowicz, Phys. Rev. Lett. **96**, 233002 (2006).
[5]R. E. Moss, Mol. Phys. **80**, 1541 (1993).
[6]A. Dalgarno, Faraday Discuss. **133**, 9 (2006).
[7]D. Galli and F. Palla, Astron. Astrophys. **335**, 403 (1998).
[8]W. Cencek, J. Rychlewski, R. Jaquet, and W. Kutzelnigg, J. Chem. Phys. **108**, 2831 (1998).
[9]L. Velilla, B. Lepetit, A. Aguado, A. Beswick, and M. Paniagua, J. Chem. Phys. **129**, 084307 (2008).
[10]D. Cappelletti, P. Candori, S. Falcinelli, M. Alberti, and F. Pirani, Chem. Phys. Lett. **545**, 14 (2012).
[11]N. Balucani, A. Bartocci, B. Brunetti, P. Candori, S. Falcinelli, F. Pirani, and F. Vecchiocattivi, Chem. Phys. Lett. **546**, 34 (2012).
[12]P. Palmieri, C. Puzzarini, V. Aquilanti, G. Capecchi, S. Cavalli, D. De Fazio, A. Aguilar, X. Giménez, and J. M. Lucas, Mol. Phys. **98**, 1835 (2000).
[13]V. Aquilanti, G. Capecchi, S. Cavalli, D. De Fazio, P. Palmieri, C. Puzzarini, A. Aguilar, X. Giménez, and J. M. Lucas, Chem. Phys. Lett. **318**, 619 (2000).
[14]T. S. Chu and K. L. Han, Phys. Chem. Chem. Phys. **10**, 2431 (2008).
[15]B. Lepetit and J. M. Launay, J. Chem. Phys. **95**, 5159 (1991).
[16]T. S. Chu, R. F. Lu, K. L. Han, X. N. Tang, H. F. Hu, and C. Y. Ng, J. Chem. Phys. **122**, 244322 (2005).
[17]X. N. Tang, C. Houchins, K. C. Lau, C. Y. Ng, R. A. Dressler, Y. H. Chiu, T. S. Chu, and K. L. Han, J. Chem. Phys. **127**, 164318 (2007).
[18]A. K. Tiwari, S. Koiakkandy, and N. Sathyamurthy, J. Phys. Chem. A **113**, 9568 (2009).
[19]A. N. Panda and N. Sathyamurthy, J. Chem. Phys. **122**, 054304 (2005).
[20]P. Tosi, R. Correale, W. Lu, S. Falcinelli, and D. Bassi, Phys. Rev. Lett. **82**, 450 (1999).
[21]T. Joseph and N. Sathyamurthy, J. Chem. Phys. **86**, 704 (1987).
[22]D. R. Mc Laughlin and D. L. Thompson, J. Chem. Phys. **70**, 2748 (1979).
[23]A. Aguado and M. Paniagua, J. Chem. Phys. **96**, 1265 (1992).

[24]S. Kumar, H. Kapoor, and N. Sathyamurthy, Chem. Phys. Lett. **289**, 361 (1998).
[25]V. Aquilanti, S. Cavalli, and D. De Fazio, J. Chem. Phys. **109**, 3792 (1998).
[26]V. Aquilanti, S. Cavalli, and G. Grossi, Chem. Phys. Lett. **110**, 43 (1984).
[27]V. Aquilanti and S. Cavalli, Chem. Phys. Lett. **141**, 309 (1987).
[28]V. Aquilanti, S. Cavalli, G. Grossi, V. Pellizzari, M. Rosi, A. Sgamellotti, and F. Tarantelli, Chem. Phys. Lett. **162**, 179 (1989).
[29]W. A. Chupka and M. E. Russel, J. Chem. Phys. **49**, 5426 (1968).
[30]X. N. Tang, H. Xu, T. Zhang, Y. Hou, C. Chang, C. Y. Ng, Y. Chiu, R. A. Dressler, and D. J. Levandier, J. Chem. Phys. **122**, 164301 (2005).
[31]C. N. Ramachandran, D. De Fazio, S. Cavalli, F. Tarantelli, and V. Aquilanti, Chem. Phys. Lett. **469**, 26 (2009).
[32]J. Zhao and Y. Luo, J. Phys. Chem. A **116**, 2388 (2012).
[33]X. G. Liu, H. Kong, W. W. Xu, J. J. Liang, F. J. Zhong, and Q. G. Zhang, THEOCHEM **908**, 117 (2009).
[34]S. Bovino, M. Tacconi, F. A. Gianturco, and D. Galli, Astron. Astrophys. **529**, A140 (2011).
[35]S. Bovino, M. Tacconi, and F. A. Gianturco, J. Phys. Chem. A **115**, 8197 (2011).
[36]H.-J. Werner, P. J. Knowles, G. Knizia, F. R. Manby, and M. Schütz *et al.*, MOLPRO, version 2010.1, a package of *ab initio* programs, 2010, see http://www.molpro.net.
[37]T. H. Dunning, J. Chem. Phys. **90**, 1007 (1989).
[38]S. Wolfram, *The Mathematica Book*, 4th ed. (Wolfram Media/Cambridge University Press, 1999).
[39]L. Velilla, M. Paniagua, and A. Aguado, Int. J. Quantum Chem. **111**, 387 (2011).
[40]M. Masili and A. F. Starace, Phys. Rev. A **68**, 012508 (2003).
[41]M. F. Falcetta, Mol. Phys. **88**, 647 (1996).
[42]M. F. Falcetta and P. E. Siska, Mol. Phys. **97**, 117 (1999).
[43]D. De Fazio, F. A. Gianturco, J. A. Rodriguez-Ruiz, K. T. Tang, and J. P. Toennies, J. Phys. B: At. Mol. Opt. Phys. **27**, 303 (1994).
[44]C. Fabri, G. Czako, G. Tasi, and A. Csaszar, J. Chem. Phys. **130**, 134314 (2009).
[45]D. W. Schwenke, J. Chem. Phys. **114**, 1693 (2001).
[46]M. Stanke, D. Kedziera, S. Bubin, and L. Adamowicz, Phys. Rev. A **77**, 022506 (2008).
[47]Z. Liu and P. B. Davies, J. Chem. Phys. **107**, 337 (1997).
[48]D. Skouteris, J. F. Castillo, and D. E. Manolopoulos, Comp. Phys. Commun. **133**, 128 (2000).
[49]D. E. Manolopoulos, J. Chem. Phys. **85**, 6425 (1986).
[50]F. D. Colavecchia, F. Mrugala, G. A. Parker, and R. T. Pack, J. Chem. Phys. **118**, 10137 (2003).
[51]D. De Fazio, J. M. Lucas, V. Aquilanti, and S. Cavalli, Phys. Chem. Chem. Phys. **13**, 8571 (2011).
[52]D. De Fazio and J. F. Castillo, Phys. Chem. Chem. Phys. **1**, 1165 (1999).
[53]D. De Fazio, V. Aquilanti, S. Cavalli, A. Aguilar, and J. M. Lucas, J. Chem. Phys. **125**, 133109 (2006).
[54]S. Kolakkandy, K. Giri, and N. Sathyamurthy, J. Chem. Phys. **136**, 244312 (2012).
[55]See supplementary material at http://dx.doi.org/10.1063/1.4772651 for numerical values of the He + $H_2^+(v = 0–5, j = 1)$ ics calculated using PM10 and RMRCI PESs and for FORTRAN subroutines of the PESs. Appendix II reporting a comparison with previous theoretical data[12,16,19] is also included.
[56]M. Baer, S. Suzuki, K. Tanaka, I. Koyano, H. Nakamura, and Z. Herman, Phys. Rev. A **34**, 1748 (1986).
[57]Z. Herman and I. Koyano, J. Chem. Soc. Faraday Trans. **83**, 127 (1987).
[58]W. A. Chupka, in *Ion-Molecule Reactions*, edited by J. L. Franklin (Plenum, New York, 1972), Vol. 1, Chap. 3, p. 72.
[59]J. C. Light, J. Chem. Phys. **41**, 586587 (1964).
[60]R. D. Levine and R. B. Bernstein, J. Chem. Phys. **56**, 2281 (1972).
[61]D. Sokolovski, S. Sen, V. Aquilanti, S. Cavalli, and D. De Fazio, J. Chem. Phys. **126**, 084305 (2007).
[62]V. Aquilanti, S. Cavalli, D. De Fazio, A. Simoni, and T. V. Tscherbul, J. Chem. Phys. **123**, 054314 (2005).
[63]D. De Fazio, S. Cavalli, V. Aquilanti, A. A. Buchacenko, and T. V. Tscherbul, J. Phys. Chem. A **111**, 12538 (2007).
[64]D. Sokolovski, D. De Fazio, S. Cavalli, and V. Aquilanti, Phys. Chem. Chem. Phys. **9**, 5664 (2007).
[65]R. D. Levine, *Molecular Reaction Dynamics* (Cambridge University Press, United Kingdom, 2005), Chap. 3.
[66]D. De Fazio, V. Aquilanti, S. Cavalli, A. Aguilar, and J. M. Lucas, J. Chem. Phys. **129**, 064303 (2008).
[67]S. Mahapatra and N. Sathyamurthy, J. Chem. Phys. **107**, 6621 (1997).
[68]Z. Darakjian, P. Pendergast, and F. E. Hayes, J. Chem. Phys. **102**, 4461 (1995).
[69]A. N. Panda and S. C. Althorpe, Chem. Phys. Lett. **419**, 245 (2006).
[70]D. Sokolovski, D. De Fazio, S. Cavalli, and V. Aquilanti, J. Chem. Phys. **126**, 121101 (2007).
[71]P. S. Jiulienne, Nat. Phys. **8**, 642 (2012).
[72]R. Rohse, W. Kutzelnigg, R. Jaquet, and W. Klopper, J. Chem. Phys. **101**, 2231 (1994).
[73]R. E. Moss, Mol. Phys. **89**, 195 (1996).
[74]R. Jaquet, Chem. Phys. Lett. **302**, 27 (1999).
[75]W. Kutzelnigg, Mol. Phys. **90**, 909 (1997); *ibid.* **105**, 2627 (2007).
[76]CODATA 2010, see http://physics.nist.gov/cuu/Constants.